RSC Advances

PAPER

View Article Online
View Journal | View Issue

Cite this: *RSC Adv.*, 2020, **10**, 33635

Fluorescent probe based on N-doped carbon dots for the detection of intracellular pH and glutathione†

Meihua Lin, Xin Ma, Shijun Lin, Xiaojin Zhang, Yu Dai* and Fan Xia

Received 31st July 2020
Accepted 31st August 2020

DOI: 10.1039/d0ra06636b

rsc.li/rsc-advances

Carbon dots (CDs) as fluorescent probes have been widely exploited to detect biomarkers, however, tedious surface modification of CDs is generally required to achieve a relatively good detection ability. Here, we synthesized N-doped carbon dots (N-CDs) from triethylenetetramine (TETA) and *m*-phenylenediamine (*m*-PD) using a one-step hydrothermal method. When the pH increases from 3 to 11, the fluorescence intensity of the N-CDs gradually decreases. Furthermore, it displays a linear response to the physiological pH range of 5–8. Au^{3+} is reduced by amino groups on the surface of N-CDs to generate gold nanoparticles (AuNPs), causing fluorescence quenching of the N-CDs. If glutathione (GSH) is then added, the fluorescence of the N-CDs is recovered. The fluorescence intensity of the N-CDs is linearly correlated with the GSH concentration in the range of 50–400 μM with a limit of detection (LOD) of 7.83 μM. The fluorescence probe was used to distinguish cancer cells from normal cells using pH and to evaluate intracellular GSH. This work expands the application of CDs in multicomponent detection and provides a facile fluorescent probe for the detection of intracellular pH and GSH.

1. Introduction

There are significant differences in the pH value and glutathione (GSH) concentration between cancer cells and normal cells.[1] The weakly acidic pH and high GSH in cancer cells have become important biomarkers to distinguish cells.[2,3] Therefore, the detection of intracellular pH and GSH is of great significance for monitoring some diseases and maintaining the normal physiological status.[4–7] As an intracellular imaging probe, fluorescent carbon dots (CDs) have attracted significant attention owing to their high photostability, excellent biocompatibility, and good specificity.[8–10] To achieve a relatively good detection ability, CDs need to be modified with functional moieties, resulting in complicated experimental operations.[11–13] Therefore, naked CDs as a fluorescent probe for the detection of intracellular pH and GSH are desired.

Recently, N,S co-doped CDs were synthesized directly from L-cysteine and $NH_3 \cdot H_2O$ using a one-step hydrothermal method.[14] The transition between C–NH_2 in acidic conditions and C=NH in alkaline conditions results in the pH-dependent switchable fluorescent properties of the N,S co-doped CDs. GSH and N,S co-doped CDs can form complexes *via* electrostatic interactions and hydrogen bonding, leading to a decrease in the fluorescence of the N,S co-doped CDs. Silver nanoparticles (AgNPs) and N,S co-doped CDs assemble an energy transfer-based quenching system and feature a pH-dependent photoluminescence "switch-on" response.[15] GSH can encapsulate AgNPs, weakening the binding of N,S co-doped CDs on the surface of the AgNPs, which can lead to photoluminescence signal recovery. Despite some progress on this, we wondered if it was possible to construct a fluorescent probe based on N-doped CDs (N-CDs) for the detection of intracellular pH and GSH.

Here, we synthesized N-CDs from triethylenetetramine (TETA) and *m*-phenylenediamine (*m*-PD) using a one-step hydrothermal method[16] and used N-CDs as a fluorescent probe for the detection of intracellular pH and GSH. N-CDs have a pH-dependent switchable fluorescent property. With the increase in pH, the fluorescence intensity of the N-CDs decreases. Amino groups on the surface of the N-CDs can reduce the Au^{3+} to generate gold nanoparticles (AuNPs), which results in fluorescence quenching of the N-CDs. With the addition of GSH, the fluorescence of the N-CDs recovers. This strategy can be applied to distinguish cancer cells from normal cells using pH and to detect intracellular GSH.

As we all know, there are few reports on the simultaneous detection of pH and GSH based on CDs. For example, N-CDs are synthesized from hexamethylenetetramine using a one-step hydrothermal method.[17] N-CDs exhibit pH-dependent optical properties. The fluorescence of the N-CDs could be effectively quenched by the Cu^{2+} and specifically recovered by GSH. The fluorescent probe based on N-CDs was applied to detect pH in

Engineering Research Center of Nano-Geomaterials of Ministry of Education, Faculty of Materials Science and Chemistry, China University of Geosciences, Wuhan 430074, China. E-mail: yudai@cug.edu.cn

† Electronic supplementary information (ESI) available. See DOI: 10.1039/d0ra06636b

the range of 2.8–7.2 and GSH with a linear range of 0.1–30 μM. As another example, N-CDs were synthesized from citric acid, polyethyleneimine, and rhodamine B using a one-step hydrothermal method.[18] The fluorescence of the N-CDs is sensitive to the pH as the intensity decreases gradually with pH. GSH can recover the fluorescence quenched by Hg^{2+}. The pH in the range of 5–10 and the GSH with a linear range of 1–10 μM were detected. Compared with these reports, our probe can detect a wide pH value (5–11) and high GSH concentration (50–400 μM).

2. Experimental

2.1. Chemicals and materials

Triethylenetetramine, *m*-PD, reduced L-glutathione (GSH, 98%), and 5,5′-dithiobis(2-nitrobenzoic acid) (DTNB) were purchased from Aladdin Chemical Reagent Co., Ltd. (Shanghai, China). Hydrochloric acid (36–38 wt%) was purchased from Sinopharm Chemical Reagent Co. Ltd. (Shanghai, China). Deionized water (18.2 MΩ cm^{-1}) was used throughout the experiments. All of the metal salts (NaCl, KCl, $Sr(NO_3)_2$, $MgCl_2$, $CaCl_2$, $AlCl_3$, $AgNO_3$, $ZnCl_2$, $Cd(NO_3)_2$, $BaCl_2$, $Mn(NO_3)_2$, $Pb(NO_3)_2$, $Hg(NO_3)_2$, $Cr(NO_3)_2$, Na_2SO_4, Na_2SO_3, Na_2CO_3, $NaNO_3$, $CuSO_4$, $FeCl_3$, and $FeCl_2$), amino acids (alanine (Ala), arginine (Arg), glutamine (Gln), glycine (Gly), histidine (His), leucine (Leu), lysine (Lys), phenylalanine (Phe), proline (Pro), threonine (Thr), tyrosine (Tyr), valine (Val), serine (Ser), tryptophan (Trp), aspartic acid (Asp), homocysteine (Hcy), and cysteine (Cys)), glucose (Glu), D-fructose (Fru) and dopamine hydrochloride (DA) were purchased from Aladdin Chemical Reagent Co. Ltd. (Shanghai, China). Gold(III) chloride trihydrate, MTT (3-(4,5-dimethylthiazol-2-yl)-2,5-diphenyltetrazolium bromide), and DiI dye (1,1′-dioctadecyl-3,3,3′,3′-tetramethylindocarbocyanine perchlorate) were purchased from Sigma-Aldrich (Shanghai, China).

2.2. Synthesis of the N-CDs

Triethylenetetramine (0.2 mL) and *m*-PD (100 mg) were dissolved in deionized water (4.8 mL), followed by heating hydrothermally at 220 °C for 24 h in a Teflon-equipped stainless-steel autoclave. Then, the reactor was naturally cooled to room temperature. The solution was separated using silica-gel column chromatography (300–400 mesh) using CH_3OH/CH_2Cl_2 (8 : 1, v/v) as eluents. After removing the solvents and further drying under a vacuum, the purified N-CDs were finally obtained.

2.3. Characterization of the N-CDs

A UV 2600 UV-Vis spectrophotometer (Shimadzu, Japan) was used to record the absorption spectrum of the N-CDs. A FS5 spectrofluorometer (Edinburgh, UK) was used to record the fluorescence spectra of the N-CDs. The slit widths of the emission and excitation were both set to 2 nm. A Zetasizer Nano ZS90 (Malvern, UK) was used to determine zeta potential of the N-CDs.

2.4. Cytotoxicity test

The *in vitro* cytotoxicity of the N-CDs against HeLa cells was tested using a MTT assay. First, the HeLa cells were seeded in a 96-well plate with a density of 1×10^4 cells per mL and incubated for 24 h at 37 °C. Then, the culture medium was removed and the cells were cultured with Dulbecco's Modified Eagle's Medium (DMEM) containing different concentrations of the N-CDs (10–150 μg mL^{-1}) for 24 h. Then, the culture media was removed and 10 μL of MTT (5.0 mg mL^{-1} in phosphate buffered saline (PBS)) was added into each well with fresh culture media. After 4 h of incubation, the culture media was removed again and 50 μL of DMSO was added into each well to dissolve the MTT. Finally, the microplate reader (Tecan, Austria) was used to record the absorbance at a wavelength of 490 nm.

2.5. Detection of pH and GSH in solution

For detection of the pH, 0.1 mL of the N-CDs solution and 1.9 mL of the phosphate buffer were added into the tubes. Then, the mixture was shaken thoroughly. The fluorescence spectra were recorded. The pH ranged from 3 to 11.

For detection of the GSH, the N-CDs solution, Au^{3+} solution, and GSH solution were added into the tubes. The mixture was diluted with deionized water to 2 mL and shaken thoroughly. The fluorescence spectra were recorded. The Au^{3+} concentration was 800 μM. The GSH concentration ranged from 0 to 1000 μM.

2.6. Determination of Au^{3+}

The samples of N-CDs + Au^{3+}, N-CDs + Au^{3+}+GSH, and Au^{3+}+GSH were configured. The concentrations of the N-CDs, Au^{3+}, and GSH were 50 mg mL^{-1}, 800 μM, and 1000 μM, respectively. The samples were then centrifuged for 5 min (8000 r per min). The supernatant fluid was put into the corresponding sample bottle and evaporated to dryness. Au^{3+} was then extracted with 3% hydrochloric acid and the volume was adjusted to 10 mL. The precipitate was transferred to the sample bottle, soaked in aqua regia, and steamed to give a wet salt. Au^{3+} was then extracted with 3% hydrochloric acid and the volume was adjusted to 10 mL. All of the test solutions were filtered through a 0.22 μm polyethersulfone (PES) membrane to remove the impurities. Three samples of the same system were prepared in parallel. The gold concentration was determined using inductively coupled plasma optical emission spectrometry (ICP-OES, Optima 5300 DV, PerkinElmer, USA).

2.7. pH sensing in living cells

The potential of the N-CDs for detecting biomarkers can be displayed using a HeLa and HESC cellular imaging study. To distinguish between the two kinds of cells, HeLa cells were incubated with DiI (5 μg mL^{-1} in DMEM) at 5% CO_2 at 37 °C for 12 h. Then, labeled HeLa and HESC cells were mixed and incubated together in DMEM at 5% CO_2 at 37 °C for 24 h. For N-CDs labeling, the above mentioned cells were incubated with the N-CDs (50 μg mL^{-1} in DMEM) at 37 °C under 5% CO_2 for different periods of time. Next, the cells were washed with PBS

three times. The images were recorded using LSM 880 confocal microscopy (Carl Zeiss).

2.8. Evaluation of GSH in HeLa cells

HeLa cells were cultured in 75 cm^2 flasks with DMEM containing a high level of glucose at 37 °C in 5% CO_2. After trypsinization, the cells were collected and washed using PBS three times. The cellular fluid was obtained using repeated freeze–thaw cycles.

The procedure for the detection of GSH in HeLa cells was the same as specified above. For comparison, Ellmann's method was employed according to the previous report.[19] The mixture comprised 0.1 mL of cell lysate, 1.9 mL of Tris-HCl buffer (0.1 M pH 8.2) and 0.1 mL Ellmann reagent (6 mg DTNB/10 mL Tris-HCl buffer). The UV-Vis absorbance of the mixture at 412 nm was recorded.

3. Results and discussion

3.1. Synthesis and characterization of the N-CDs

The N-CDs were synthesized from *m*-PD and TETA using a one-pot hydrothermal method according to a method reported previously.[16] Amino groups are abundant on the surface of the N-CDs (Fig. 1a). As a result, the N-CDs have a zeta potential of 28.1 ± 0.3 mV (Fig. 1b). The N-CDs are nanoparticles in the range of 2–4 nm characterized using transmission electron microscopy (TEM) (Fig. S1†). The N-CDs exhibit a good solubility and stability in water. The N-CDs solution can be stored at 4 °C for several months. UV-Vis absorption of the N-CDs shows an absorption band at 289 nm (Fig. S2†), which is ascribed to the presence of π–π* (C=C) and *n*–π (C–N) transitions.[20] With the increase in the excitation wavelength from 380 to 420 nm, the fluorescence intensity of the N-CDs shows a slight change, demonstrating excitation-dependent behavior (Fig. 1c).[21] The fluorescence emission of the N-CDs excited at 400 nm is relatively strong. Thus, excitation at 400 nm is used throughout the experiments. The quantum yield of the N-CDs is 6%. In addition, the N-CDs possess a low toxicity (Fig. 1d).

The effect of the solution conditions on the fluorescence stability of the N-CDs was investigated. The fluorescence intensity of the N-CDs was stable at different temperatures (Fig. S3†). The N-CDs were stable at different temperatures. The fluorescence intensity of the N-CDs does not change significantly with NaCl concentrations ranging from 0 to 0.8 M (Fig. S4†). The results show that the N-CDs possess an outstanding fluorescence stability when the temperature and NaCl concentration of the N-CDs solution change within a certain range.

3.2. Detection of pH in solution

Several experimental conditions that may affect the sensitivity were optimized prior to the application, including the buffer solution and the concentration of N-CDs. First, we selected a citrate buffer (Fig. S5†), Tris-HCl buffer (Fig. S6†), HCl/NaOH solution (Fig. S7†), and PBS buffer (Fig. 2a and b) as the research objects. With the increase in the pH, the fluorescence intensity of the N-CDs decreased in all buffers. However, the magnitude of the fluorescence quenching and the pH response range was different. The fluorescence quenching rates were low in the citrate buffer, Tris-HCl buffer, and HCl/NaOH solution, but high in the PBS buffer, which was 73.7%. When the pH was higher than 5, the fluorescence intensity began to significantly respond to the pH in the PBS buffer, changing less in the other buffers. Therefore, we chose the PBS buffer for use in subsequent experiments. Then, we studied the effect of the concentration of N-CDs on the fluorescence intensity of the N-CDs

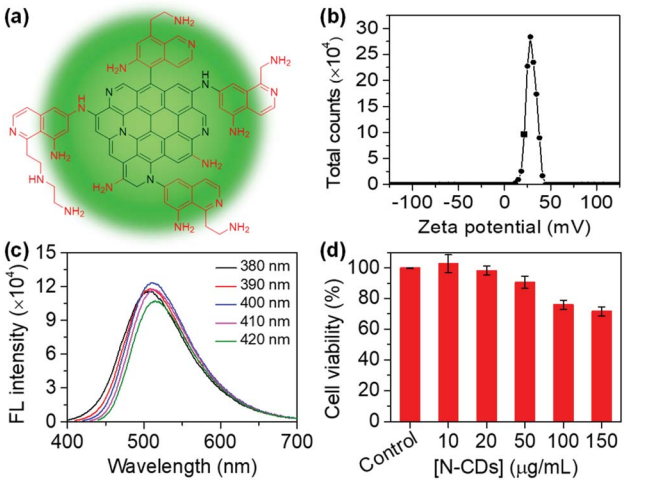

Fig. 1 Structure and properties of the N-CDs. (a) Structural formula of the N-CDs. (b) Zeta potential of the N-CDs. (c) Fluorescence emission spectra of the N-CDs under different excitation wavelengths (from 380 to 420 nm). (d) Cytotoxicity of the N-CDs toward HeLa cells assessed using an MTT assay.

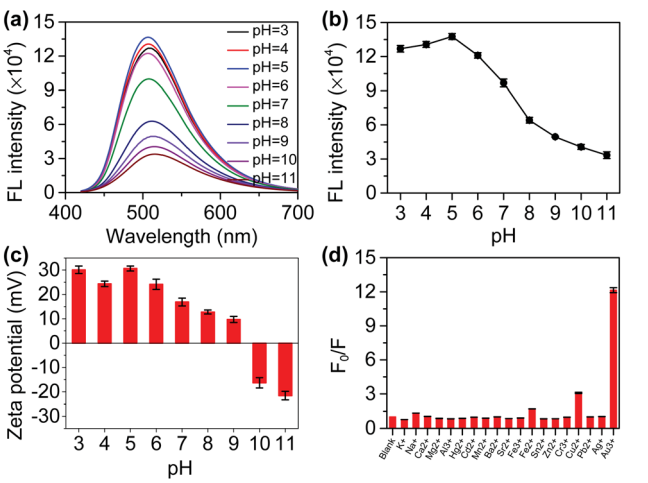

Fig. 2 Detection of pH in solution. (a) Fluorescence spectra of the N-CDs as the pH increases from 3 to 11. Ex = 400 nm, Em = 510 nm. (b) Relationship between the fluorescence intensity at 510 nm and the pH. (c) Zeta potential of the N-CDs at different pH values. (d) Selectivity of the probe towards metal ions at pH 7. F_0 and F represent the fluorescence intensity of the N-CDs and N-CDs + analyte at 510 nm, respectively. The analyte concentration is 1 mM. Ex = 400 nm. All experiments were repeated three times.

(Fig. S8†). If the concentration of N-CDs is 0.2%, 0.5%, or 1%, the fluorescence intensity of the N-CDs is low and changes less with pH. When N-CDs concentration is 5%, the fluorescence intensity of the N-CDs is high and the tendency to change with pH is also high. When the concentration of N-CDs is higher, the fluorescence intensity of the N-CDs changes slightly and the trend is similar to that at a concentration of 5% N-CDs. Therefore, we chose a N-CDs concentration of 5% in the subsequent experiments.

The fluorescence emission spectra of the N-CDs at different pH values were recorded. With the increase in pH, the fluorescence intensity of the N-CDs at 510 nm gradually decreases (Fig. 2a). There is a relationship between the fluorescence intensity and pH (Fig. 2b). Furthermore, there is a good linear relationship between the fluorescence intensity and the pH in the range of 5–8 and 8–11 (Fig. S9†). Photographs of the N-CDs in the different pH PBS solutions under daylight and UV lamp (365 nm) irradiation were taken (Fig. S10†). Interestingly, as the pH drops from 11 to 3, the light yellow color of the N-CDs solution gradually becomes deeper under daylight and a gradual increase in the fluorescence can also be observed with the naked eye, and the fluorescence shows a significant difference between the weakly alkaline and weakly acidic conditions.

The N-CDs aggregate when the pH increases (Fig. S11†). It is possible that the N-CDs self-assemble into larger particles when the pH is adjusted from acidic to alkaline solutions. With pH increases from 3 to 11, the zeta potential of the N-CDs solution changes from a positive to a negative charge (Fig. 2c). A sufficient number of amino groups on the surface of the N-CDs can form a positively charged surface because the pKa value of the amino groups varies between 9 and 10.[22] Under highly acidic conditions (pH 3.0), a corrected value of +30.4 mV is observed, which is consistent with the positively charged $-NH_3^+$ group on the surface of the N-CDs. In short, the zeta potential measurements of the N-CDs in strongly acidic media indicate that the $-NH_2$ groups are protonated by pH, which can counteract aggregation by electrostatic repulsion.[23] In contrast, in an alkaline solution (pH 10), the zeta potential is −16.3 mV, and the N-CDs are partially deprotonated, in which the fluorescence is mostly quenched. Meanwhile, it was found that as the pH increases, the monodisperse N-CDs are converted into nanoaggregates, resulting in weaker fluorescence at a higher pH.[24] Therefore, the as-prepared N-CDs are a potential pH probe and could act as biosensing platforms to distinguish cancer cells from normal cells owing to the pH difference in cells.[25]

To test the selectivity of the probe, analytes such as Na^+, K^+, Sr^{2+}, Mg^{2+}, Ca^{2+}, Al^{3+}, Ag^+, Zn^{2+}, Cd^{2+}, Ba^{2+}, Mn^{2+}, Pb^{2+}, Hg^{2+}, Cr^{2+}, Sn^{2+}, Au^{3+}, Fe^{3+}, and Fe^{2+} were chosen. The fluorescence intensity of the N-CDs showed no obvious change at different pH values except for Au^{3+} (Fig. 2d and S12†). This is an interesting result that will be further applied for the detection of GSH in subsequent experiments.

3.3. pH sensing for distinguishing cells

To distinguish cancer cells (HeLa) from normal cells (HESC), we selected DiI to stain HeLa cells as its fluorescence emission is

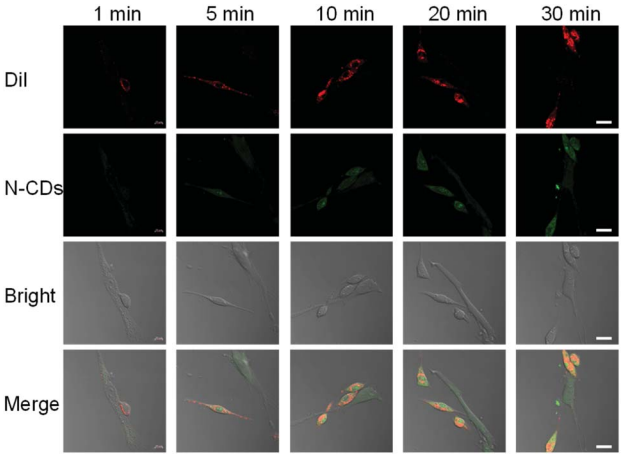

Fig. 3 Confocal images of co-cultured DiI-labeled HeLa and HESC cells with N-CDs. Ex = 544 nm, Em = 555–575 nm. Scale bar: 20 μm.

565 nm, which does not overlap with the fluorescence peaks of the N-CDs.[26] The staining can be traced for a long time, which is convenient for cell co-culturing. First, the HeLa cells were stained with DiI. Then, the cells were washed with PBS and co-cultured with HESC cells. Finally, confocal microscopy was used to take pictures. DiI can distinguish two types of cells by staining only HeLa cells (Fig. S13†). Only HeLa cells have a red fluorescence and HESC cells have no fluorescence. At the same time, DiI retains the red fluorescence after 48 h, proving that a long-term incubation does not affect its ability to discriminate between the two cells.

After that, we incubated the two cells with N-CDs and observed the fluorescence intensity of the N-CDs in different cells. The confocal images of the N-CDs after different incubation times were recorded (Fig. 3). For 1 min incubation, the green fluorescence in cells is weak. When the cells are incubated for 5 min or longer, more N-CDs enter the cells and the fluorescence intensity increases. With the increase in incubation time, the green fluorescence of the N-CDs in the HeLa cells with the red fluorescent of DiI is also relatively strong, which proves that the fluorescence intensity of the N-CDs in HeLa cells is higher than that in HESC cells. This is due to the pH of 7.4 in normal cells and the acidic environment in cancer cells.[27] Therefore, this phenomenon is consistent with the strong fluorescence of the N-CDs in an acidic environment and a weak fluorescence in an alkaline environment, and the N-CDs can be used as a potential pH probe to distinguish cancer cells from normal cells.

3.4. Detection of GSH in solution

The addition of Au^{3+} significantly quenches the fluorescence of the N-CDs, which can be recovered after GSH is added (Fig. 4a). GSH has no significant effect on the fluorescence of the N-CDs. Therefore, an "on–off–on" fluorescent probe based on N-CDs could be built to detect GSH. We first performed optimization on the temperature, incubation time, and Au^{3+} or N-CDs concentration. The Au^{3+} concentration is closely related to the

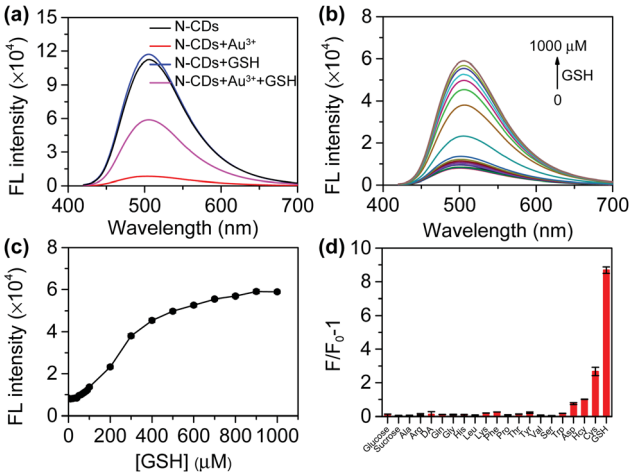

Fig. 4 Detection of GSH in solution. (a) Fluorescence spectra of the N-CDs, N-CDs + Au^{3+}, N-CDs + GSH, and N-CDs + Au^{3+} + GSH. (b) Fluorescence spectra of the N-CDs + Au^{3+} with the addition of GSH (0, 10, 20, 30, 40, 50, 60, 70, 80, 90, 100, 200, 300, 400, 500, 600, 700, 800, 900, and 1000 μM). (c) Relationship between the fluorescence intensity at 510 nm and the GSH concentration. (d) Selectivity of the probe towards biological molecules. F_0 and F represent the fluorescence intensity of N-CDs + Au^{3+} and N-CDs + Au^{3+} + analyte at 510 nm, respectively. All experiments were repeated three times.

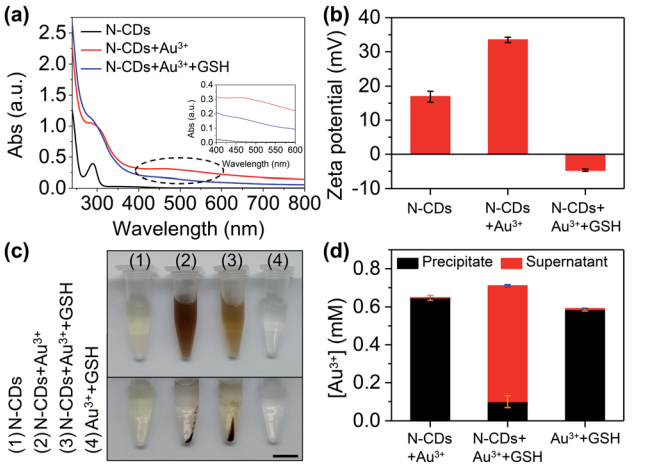

Fig. 5 Mechanism investigation. (a) UV-Vis absorption of the N-CDs, N-CDs + Au^{3+}, and N-CDs + Au^{3+}+GSH. The inset graph shows an enlarged view of the 400 to 600 nm range. (b) Zeta potential of the N-CDs, N-CDs + Au^{3+}, and N-CDs + Au^{3+} + GSH. (c) Photographs of the N-CDs, N-CDs + Au^{3+}, N-CDs + Au^{3+} + GSH, and Au^{3+} + GSH. Scale bar: 1 cm. (d) Gold concentration in the precipitate and supernatant calculated from the ICP-OES data.

quenching efficiency (Fig. S14†). Considering the quenching efficiency and recovery efficiency, 800 μM of Au^{3+} was chosen (Fig. S15†). The fluorescence of the N-CDs was quenched by approximately 90.9% and changed slightly upon further increasing the Au^{3+} concentration. Furthermore, the difference in the fluorescence intensity between the quenching and recovery was significant. The probe is not sensitive to temperature (Fig. S16†). The fluorescence of the N-CDs quenches within 10 s and is restored within 3 min (Fig. S17†).

Under the optimized conditions, the fluorescence recovery of the probe with the GSH concentration was investigated. The fluorescence intensity of N-CDs at 510 nm gradually increases with the increase in GSH (Fig. 4b). The relationship between the fluorescence intensity and GSH concentration is presented in Fig. 4c. A good linear relationship was obtained when the GSH concentrations range from 50–400 μM (Fig. S18†). The limit of detection (LOD) for GSH is 7.83 μM. The LOD was calculated as the ratio of the sample intensity to three standard deviations of the blank intensity.

To test the selectivity of the probe, analytes such as thiol and biological molecules were chosen. Saccharides and non-thiol amino acids do not cause a significant change in the fluorescence intensity (Fig. 4d). Although homocysteine (Hcy) and cysteine (Cys) cause fluorescence recovery, the effect of these two amino acids is much smaller than that of GSH. Meanwhile, 90% of the thiols in the cells are GSH.[28] Therefore, the probe can selectively detect GSH.

3.5. Mechanism of the "on–off–on" fluorescent probe

The mechanism of the probe was investigated. After adding Au^{3+}, an absorption peak at 490 nm appears (Fig. 5a) and the zeta potential increases (Fig. 5b), which is attributed to the formation of the gold nanoparticles (AuNPs) that are derived from the reduction of Au^{3+} by amino groups on the surface of the N-CDs.[29] AuNPs cause fluorescence quenching of the N-CDs owing to fluorescence resonance energy transfer (FRET). GSH contains a mercapto group in the molecular structure and its isoelectric point is 5.93. The zeta potential of GSH at pH 7.4 is negative.[30] With the addition of GSH, the strong affinity of GSH to AuNPs enables encapsulation of the AuNPs by GSH and improves the solution stability of the AuNPs, resulting in a reduced zeta potential (Fig. 5b).[31] The inter-particle distance is enlarged, which subsequently produces fluorescence recovery (Fig. 5a).

To further confirm the formation of AuNPs, we collected the precipitate and supernatant from the samples. The gold concentration was determined using ICP-OES. The precipitate was found in the N-CDs + Au^{3+} sample after centrifugation (Fig. 5c) and the ICP-OES data also shows a high gold concentration in the precipitate (99.9% of the total gold concentration) (Fig. 5d). When GSH is added into the N-CDs + Au^{3+} solution, the red wine color becomes faint (Fig. 5c) and the gold concentration in the precipitate is low because of the improved solution stability of the AuNPs as a result of GSH (Fig. 5d). In addition, the Au^{3+} + GSH sample was also studied. The precipitate was found after centrifugation (Fig. 5c) and the ICP-OES data showed that the Au^{3+} concentration in the precipitate accounts for 98% (Fig. 5d). It turns out that Au^{3+} can be reduced by GSH to form AuNPs.[32] Therefore, the mechanism of the "on–off–on" fluorescent probe is shown in Fig. 6a.

3.6. Detection of GSH in HeLa cells

To test the analytical ability for practical applications, the intracellular GSH concentration was detected using the probe.

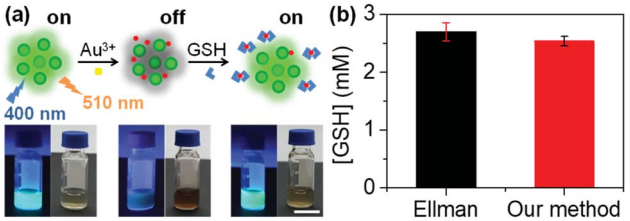

Fig. 6 Mechanism and application. (a) Schematic illustration of the mechanism. Photographs show the solutions of N-CDs, N-CDs + Au^{3+}, and N-CDs + Au^{3+} + GSH under daylight and UV lamp (365 nm) irradiation. (b) GSH concentration in HeLa cells detected using Ellman's method and our method.

Cellular fluid was obtained by repeated freeze–thaw cycles and the GSH concentration in the cellular fluid was detected. By referring to the standard curve (Fig. S18†), the GSH concentration in HeLa cells was calculated to be 2.53 ± 0.08 mM using our method (Fig. 6b). The result is in agreement with the normal level reported previously (0.5–10 mM).[33] To confirm the accuracy of our method, Ellman's method was applied to detect the intracellular GSH.[19] By referring to the standard curve, the GSH concentration in HeLa cells was found to be 2.70 ± 0.15 mM, which is close to the value obtained using our method. Although our method could not easily distinguish GSH from other biothiols, it could give information about the intracellular GSH because over 90% of the biothiols in cells are GSH.[28]

4. Conclusions

An N-CDs-based fluorescent probe was developed for the detection of pH and GSH. N-CDs were synthesized using a hydrothermal method. N-CDs show green fluorescence, excellent solubility and a good stability in water. The fluorescence intensity of N-CDs is pH-dependent with a good linear relationship for pH ranging from 5–8 and 8–11. The fluorescence of the N-CDs was quenched by AuNPs owing to the reduction of Au^{3+}. Upon the addition of GSH into the N-CDs + Au^{3+} solution, the fluorescence of the N-CDs was recovered, which is attributed to the dissociation of the AuNPs from the surface of the N-CDs driven by the strong affinity of GSH to AuNPs. N-CDs have been used to distinguish cancer cells from normal cells by pH and evaluate the intracellular GSH. This work expands the application of N-CDs in multicomponent detection and provides a facile strategy for the detection of intracellular pH and GSH.

Conflicts of interest

There are no conflicts to declare.

Acknowledgements

This work was financially supported by the National Natural Science Foundation of China (No. 51703209 and 21804122) and the Fundamental Research Funds for the Central Universities, China University of Geosciences (Wuhan) (CUG170660).

Notes and references

1 J. Y. Wu, J. Chen, Y. J. Feng, H. Y. Tian and X. S. Chen, *J. Gene Med.*, 2019, **21**, e3088.
2 Y. H. Zhan, X. J. Li, R. Sun, Y. J. Xu and J. F. Ge, *Anal. Chim. Acta*, 2016, **933**, 175–181.
3 N. Kannan, L. V. Nguyen, M. Makarem, Y. F. Dong, K. Shih, P. Eirew, A. Raouf, J. T. Emerman and C. J. Eaves, *Proc. Natl. Acad. Sci. U. S. A.*, 2014, **111**, 7789–7794.
4 C. S. Lim, G. Masanta, H. J. Kim, J. H. Han, H. M. Kim and B. R. Cho, *J. Am. Chem. Soc.*, 2011, **133**, 11132–11135.
5 B. Y. Chu, T. T. Qi, J. F. Liao, J. R. Peng, W. T. Li, S. Z. Fu, F. Luo and Z. Y. Qian, *Sens. Actuators, B*, 2012, **166**, 56–60.
6 H. Zhang, C. X. Wang, K. Wang, X. P. Xuan, Q. Z. Lv and K. Jiang, *Biosens. Bioelectron.*, 2016, **85**, 96–102.
7 J. F. Li, P. C. Huang and F. Y. Wu, *Sens. Actuators, B*, 2017, **240**, 553–559.
8 Y. Liu, M. R. Zhang, Y. F. Wu, R. Zhang, Y. Cao, X. Q. Xu, X. Chen, L. L. Cai and Q. Xu, *Chem. Commun.*, 2019, **55**, 12164–12167.
9 Q. Xu, W. J. Li, L. Ding, W. J. Yang, H. H. Xiao and W. J. Ong, *Nanoscale*, 2019, **11**, 1475–1504.
10 H. Ali, S. Ghosh and N. R. Jana, *Wiley Interdiscip. Rev.: Nanomed. Nanobiotechnol.*, 2020, **12**, e1617.
11 F. K. Du, Y. H. Min, F. Zeng, C. M. Yu and S. Z. Wu, *Small*, 2014, **10**, 964–972.
12 W. J. Liu, C. Li, Y. J. Ren, X. B. Sun, W. Pan, Y. H. Li, J. P. Wang and W. J. Wang, *J. Mater. Chem. B*, 2016, **4**, 5772–5788.
13 F. Y. Yan, Y. X. Jiang, X. D. Sun, Z. J. Bai, Y. Zhang and X. G. Zhou, *Microchim. Acta*, 2018, **185**, 424.
14 Z. Q. Song, F. Y. Quan, Y. H. Xu, M. L. Liu, L. Cui and J. Q. Liu, *Carbon*, 2016, **104**, 169–178.
15 F. Xiang, J. Z. Li and Z. D. Liu, *Analyst*, 2019, **144**, 7057–7063.
16 Y. Y. Cheng, C. M. Li, R. Z. Mu, Y. F. Li, T. T. Xing, B. B. Chen and C. Z. Huang, *Anal. Chem.*, 2018, **90**, 11358–11365.
17 S. Liao, X. Q. Huang, H. Yang and X. Q. Chen, *Anal. Bioanal. Chem.*, 2018, **410**, 7701–7710.
18 J. P. Wang, X. Y. Wang, X. H. Pan, W. Pan, Y. Li, X. Y. Liang and X. B. Sun, *Microchim. Acta*, 2020, **187**, 330.
19 J. J. Gu, D. H. Hu, W. N. Wang, Q. H. Zhang, Z. Meng, X. D. Jia and K. Xi, *Biosens. Bioelectron.*, 2015, **68**, 27–33.
20 A. A. Ensafi, S. H. Sefat, N. Kazemifard, B. Rezaei and F. Moradi, *Sens. Actuators, B*, 2017, **253**, 451–460.
21 S. J. Zhu, Q. N. Meng, L. Wang, J. H. Zhang, Y. B. Song, H. Jin, K. Zhang, H. C. Sun, H. Y. Wang and B. Yang, *Angew. Chem., Int. Ed.*, 2013, **52**, 3953–3957.
22 X. H. Wang, K. G. Qu, B. L. Xu, J. S. Ren and X. G. Qu, *J. Mater. Chem.*, 2011, **21**, 2445–2450.
23 T. Fiuza, G. Gomide, A. F. C. Campos, F. Messina and J. Depeyrot, *C–Journal of Carbon Research*, 2019, **5**, 74.
24 X. X. Ye, Y. H. Xiang, Q. R. Wang, Z. Li and Z. H. Liu, *Small*, 2019, **15**, 1901673.
25 M. Pirsaheb, S. Mohammadi and A. Salimi, *TrAC, Trends Anal. Chem.*, 2019, **115**, 83–99.

26 D. X. Liu, P. Guo, C. McCarthy, B. Wang, Y. Tao and D. Auguste, *Nat. Commun.*, 2018, **9**, 2612.
27 A. Alikhani, M. Gharooni, H. Moghtaderi, F. Farokhmanesh, H. Abiri, M. Salimi, F. Attari and M. Abdolahad, *Anal. Biochem.*, 2018, **561**, 1–10.
28 J. H. Lee, C. S. Lim, Y. S. Tian, J. H. Han and B. R. Cho, *J. Am. Chem. Soc.*, 2010, **132**, 1216–1217.
29 T. T. Yang, F. Cai, X. D. Zhang and Y. M. Huang, *RSC Adv.*, 2015, **5**, 107340–107347.
30 W. J. Dong, R. P. Wa, X. J. Gong and C. Dong, *Anal. Bioanal. Chem.*, 2019, **411**, 6687–6695.
31 Y. P. Shi, Y. Pan, H. Zhang, Z. M. Zhang, M. J. Li, C. Q. Yi and M. S. Yang, *Biosens. Bioelectron.*, 2014, **56**, 39–45.
32 X. Mao, Z. P. Li and Z. Y. Tang, *Front. Mater. Sci.*, 2011, **5**, 322–328.
33 F. G. Ottaviano, D. E. Handy and J. Loscalzo, *Circ. J.*, 2008, **72**, 1–16.